Electronic Supplementary Material (ESI) for Journal of Materials Chemistry

Ultrasensitive Sorption Behavior of Isostructural Lanthanide-Organic Frameworks Induced by Lanthanide Contraction

Zhongjun Lin [a], Ruqiang Zou [a,*], Wei Xia [a], Liangjie Chen [a], Xidong Wang [a], Fuhui Liao [b], Yingxia Wang [b], Jianhua Lin [b], Anthony K. Burrell [c]

[a] *College of Engineering, Peking University, Beijing 100871, China. E-mail: rzou@pku.edu.cn.* [b] *College of Chemistry and Molecule Engineering, Peking University, Beijing 100871, China.* [c] *Chemical Sciences and Engineering Division, Argonne National Laboratory, 9700 S. Cass Avenue, Argonne, IL 60439.*

Table S1. Crystallographic Data and Structural Refinement Summary for **Pr-LOF.**

Formula	$PrC_{33}H_{33}N_2O_{10}$
Molecular weight	758.52
T（K）	293(2)
Crystal system	hexagonal
space group	$P\,6_122$
a (Å)	16.4393(3)
b (Å)	16.4393(3)
c (Å)	23.7770(9)
Volume (Å^3)	5564.9(3)
α (deg)	90
β (deg)	90
γ (deg)	120
Z	6
ρ (g/m^3)	1.32559
R1, wR2 [I>2σ(I)]	0.0486, 0.1455

$R_1=\sum||F_o|-|F_c||/|F_o|$. $wR_2=[\sum w(F_o^2 - F_c^2)^2/\sum w(F_o^2)^2]^{1/2}$.

Table S2. Selected bond lengths (Å) and angles (°) of complex **Pr-LOF.**

Pr(1) -O(3)#1	2.371(5)	Pr(1)-O(2)#5	2.505(6)
Pr(1)-O(3)#2	2.371(5)	Pr(1)-O(1W)	2.478(9)
Pr(1)-O(2)#3	2.468(5)	Pr(1)-O(1)	2.707(5)
Pr(1)-O(2)#4	2.468(5)	Pr(1)-O(2)	2.505(6)
Pr(1)-O(1)#5	2.707(5)		
O(3)#1-Pr(1)-O(3)#2	76.5(3)	O(1)#4-Pr(1)-O(2)	95.5(3)
O(3)#1-Pr(1)-O(1)#3	136.1(2)	O(1W)-Pr(1)-O(2)	74.43(17)
O(3)#2-Pr(1)-O(1)#3	72.92(19)	O(2)#5-Pr(1)-O(2)	148.9(3)
O(3)#1-Pr(1)-O(1)#4	72.92(19)	O(3)#1-Pr(1)-O(1)#5	74.65(17)
O(3)#2-Pr(1)-O(1)#4	136.1(2)	O(3)#2-Pr(1)-O(1)#5	79.65(18)
O(1)#3-Pr(1)-O(1)#4	148.5(2)	O(1)#3-Pr(1)-O(1)#5	69.46(19)
O(3)#1-Pr(1)-O(1W)	141.74(16)	O(1)#4-Pr(1)-O(1)#5	120.30(16)
O(3)#2-Pr(1)-O(1W)	141.74(17)	O(1W)-Pr(1)-O(1)#5	106.43(12)
O(1)#3-Pr(1)-O(1W)	74.24(12)	O(2)#5-Pr(1)-O(1)#5	49.38(19)
O(1)#4-Pr(1)-O(1W)	74.24(12)	O(2)-Pr(1)-O(1)#5	143.4(3)
O(3)#1-Pr(1)-O(2)#5	79.0(3)	O(3)#1-Pr(1)-O(1)	79.65(18)
O(3)#2-Pr(1)-O(2)#5	127.7(2)	O(3)#2-Pr(1)-O(1)	74.65(17)
O(1)#3-Pr(1)-O(2)#5	95.5(3)	O(1)#3-Pr(1)-O(1)	120.30(16)
O(1)#4-Pr(1)-O(2)#5	76.0(2)	O(1)#4-Pr(1)-O(1)	69.46(19)
O(1W)-Pr(1)-O(2)#5	74.43(17)	O(1W)-Pr(1)-O(1)	106.43(12)
O(3)#1-Pr(1)-O(2)	127.7(2)	O(2)#5-Pr(1)-O(1)	143.4(3)
O(3)#2-Pr(1)-O(2)	79.0(3)	O(2)-Pr(1)-O(1)	49.38(19)
O(1)#3-Pr(1)-O(2)	76.0(2)	O(1)#5-Pr(1)-O(1)	147.1(2)

[a] Symmetry transformations used to generate equivalent atoms: #1 x+1,y+1,z; #2 x-y+1,-y+1,-z; #3 y,-x+y+1,z-1/6; #4 x,x-y+1,-z+1/6; #5 x-y+1,-y+2,-z; #6 x,x-y,-z+1/6; #7 x-y+1,x,z+1/6; #8 x-1,y-1,z.

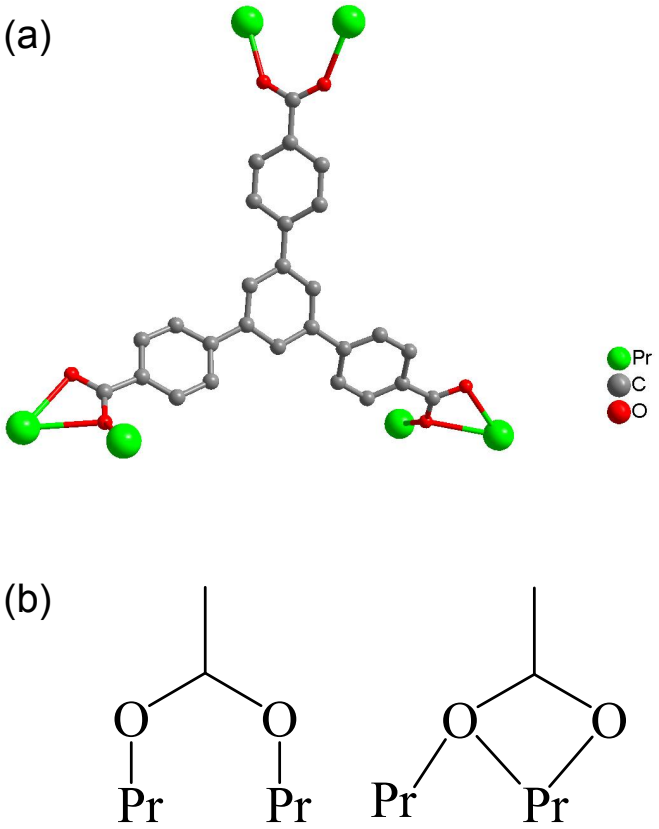

Figure S1. (a) The coordination environment of BTB ligand. (b) The two types of binding modes of BTB ligand.

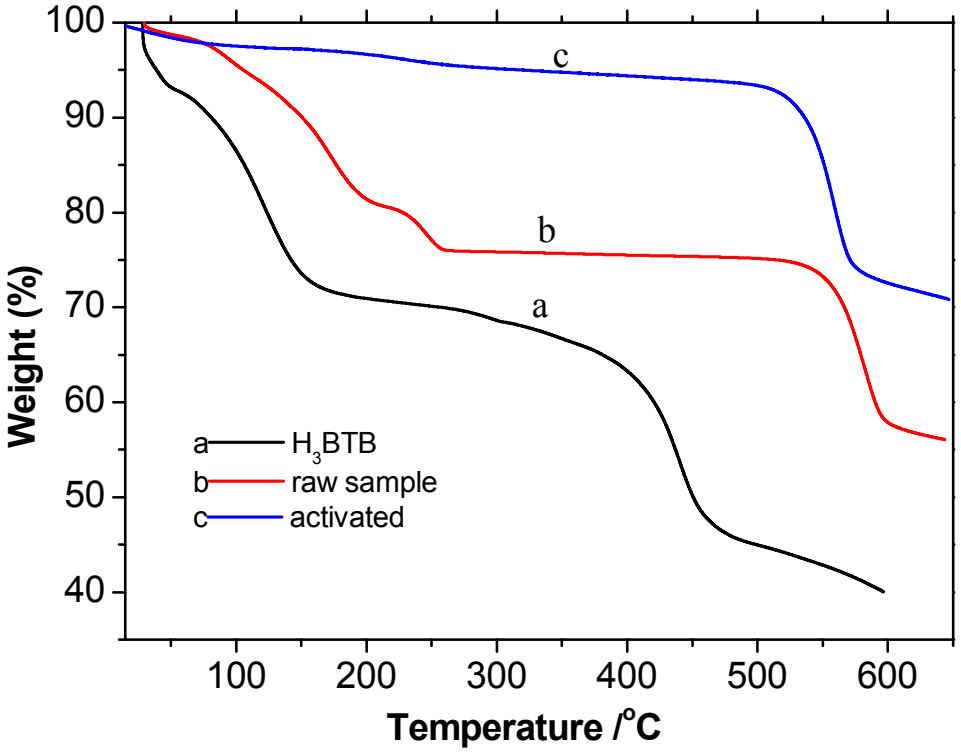

Figure S2. TG curves of H_3BTB, raw sample and activated sample of **Pr-LOF**.

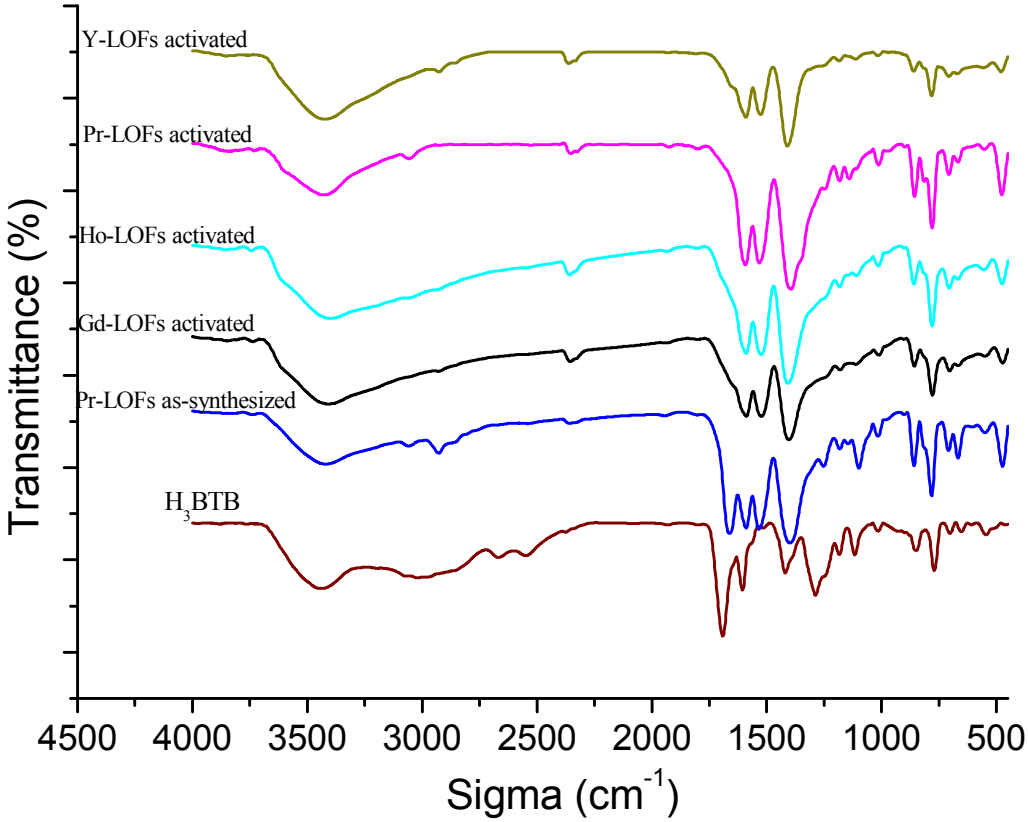

Figure S3. FTIR spectra of the as-synthesized and activated LOFs samples.

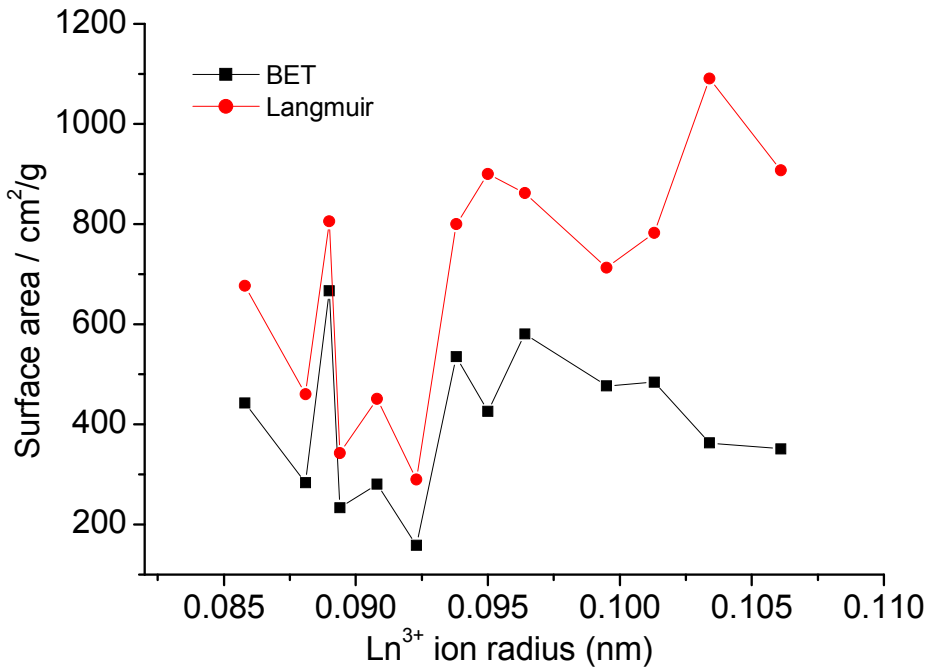

Figure S4. Relationship between ion radius and surface area.

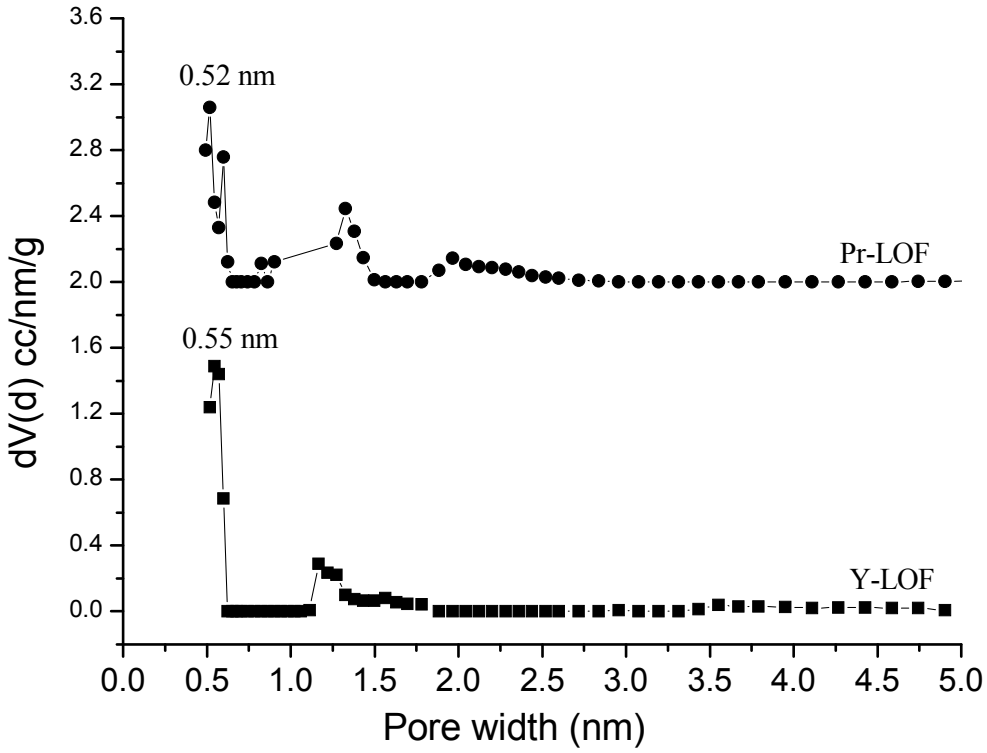

Figure S5. Pore size distribution of **Pr-LOF** and **Y-LOF** calculated by DFT method. Calc. Model: N_2 at 77 K on carbon (slit/cylinder pore, NLDFT equilibrium model).

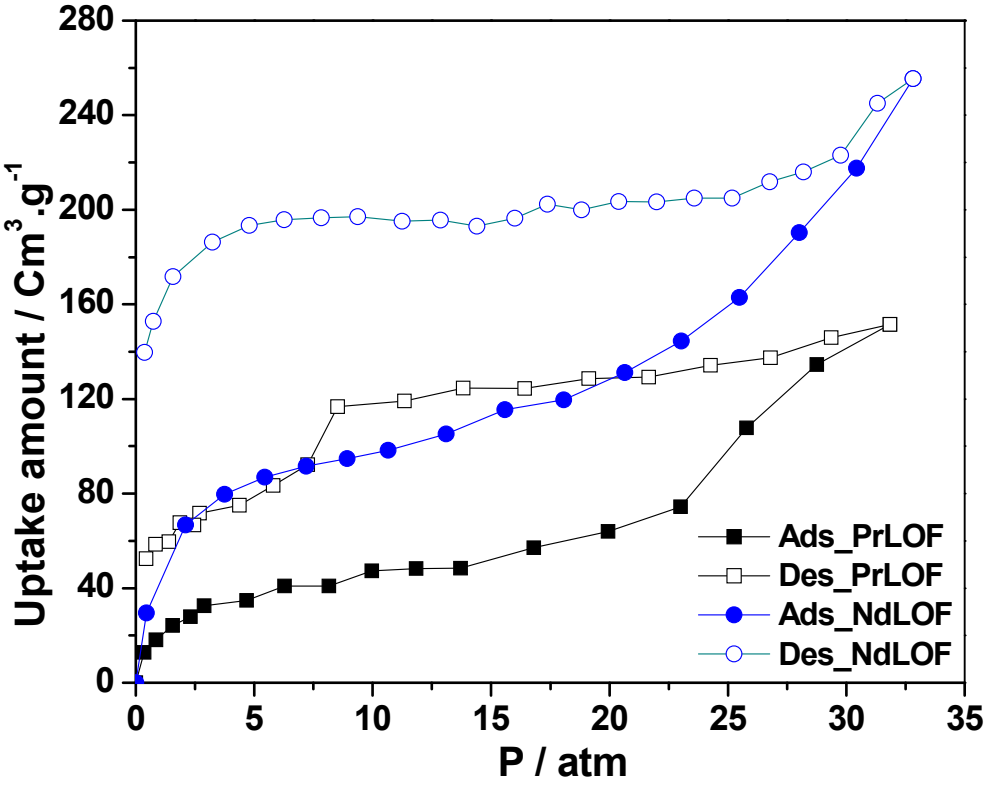

Figure S6. High pressure CO_2 adsorption (filled shapes) and desorption (open shapes) isotherms for **PrLOF** and **NdLOF** at 273 K.

The selectivity of CO_2/N_2, CH_4/N_2 and CO_2/CH_4 for **Pr-LOF** were calculated from the Henry constants. The experimental adsorption isotherms were analyzed by using single Langmuir isotherms [Eq (1)].

$$V = \frac{V_1 K_1 P}{1 + K_1 P} \qquad (1)$$

V, the total volume adsorbed of gas; P, the applied pressure; V_1, calculated adsorbed volume of CH_4; K_1, calculated affinity constants;

Fitting of the adsorption branch for CO_2, CH_4 and N_2 based on the Langmuir isotherm model allowed us to calculate the Henry constants, $H=K_1 \times V_1$.

The Henry law selectivity for gas i over gas j is then expressed by Equation:

$$S_{i/j} = \frac{H_i}{H_j} \qquad (2)$$

The fitting results are showed in Figure S7-S9.

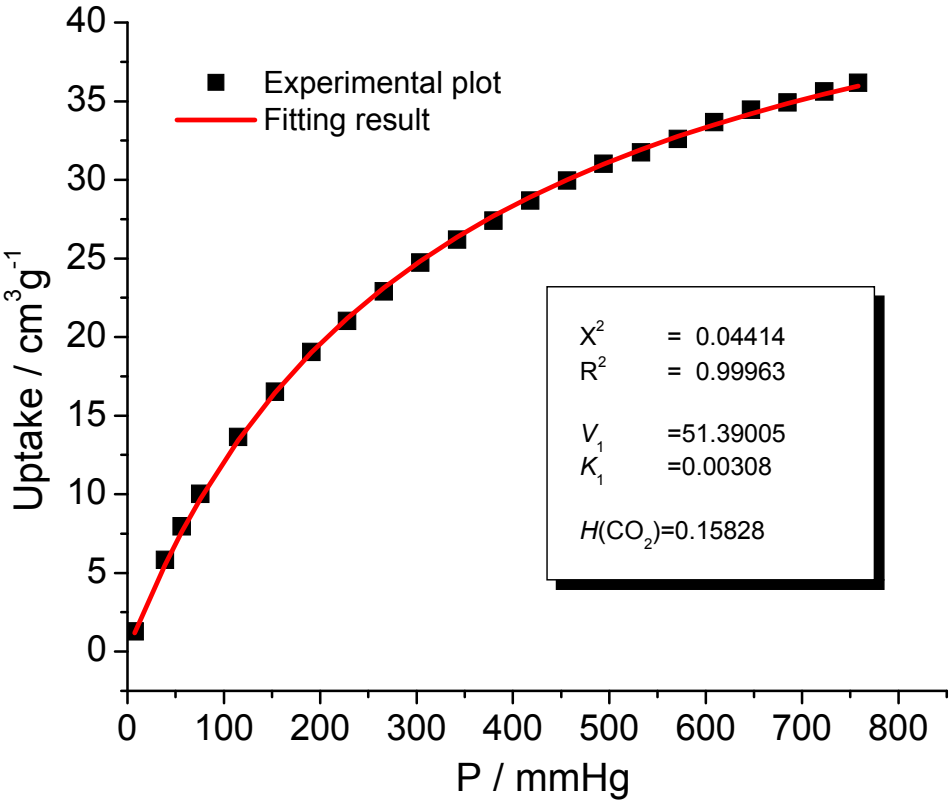

Figure S7. CO_2 isotherm adsorption branch of **Pr-LOF** (filled shape) and fitting based on single Langmuir isotherm model (red line). V_1, calculated adsorbed volume of CO_2; K_1, calculated affinity constants; X^2 and R^2, fitting error; H, Herry's law constant, $H(CO_2)=K_1\times V_1$ ($cm^3\cdot g^{-1}\cdot mmHg^{-1}$).

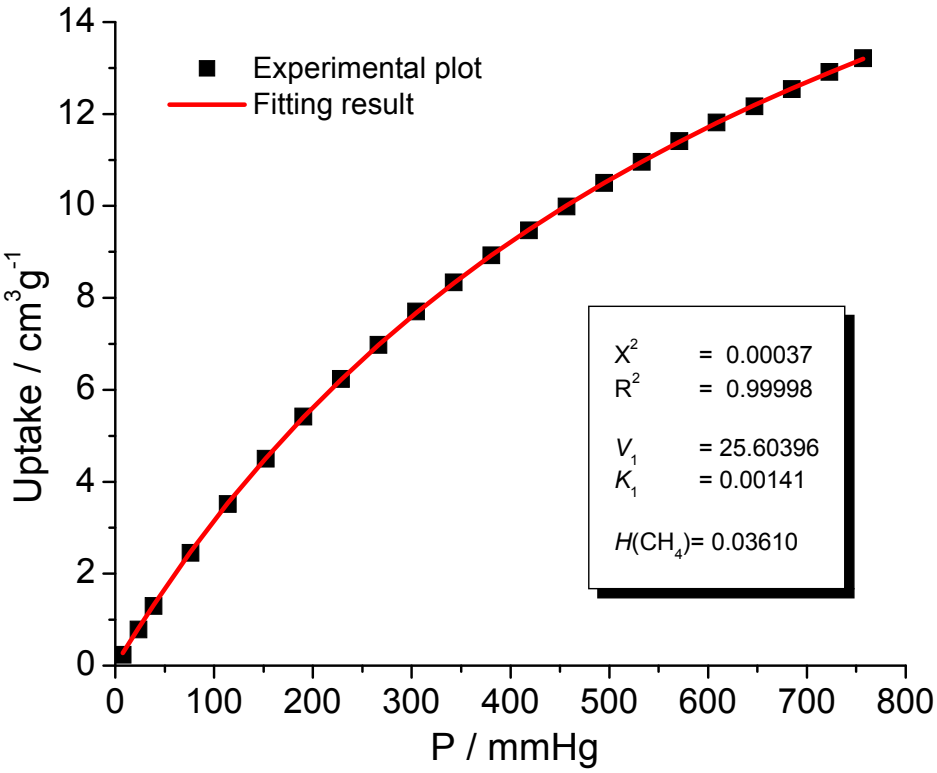

Figure S8. CH_4 isotherm adsorption branch of **Pr-LOF** (filled shape) and fitting based on single Langmuir isotherm model (red line). V_1, calculated adsorbed volume of CH_4; K_1, calculated affinity constants; X^2 and R^2, fitting error; H, Herry's law constant, $H(CH_4)=K_1\times V_1$ ($cm^3\cdot g^{-1}\cdot mmHg^{-1}$).

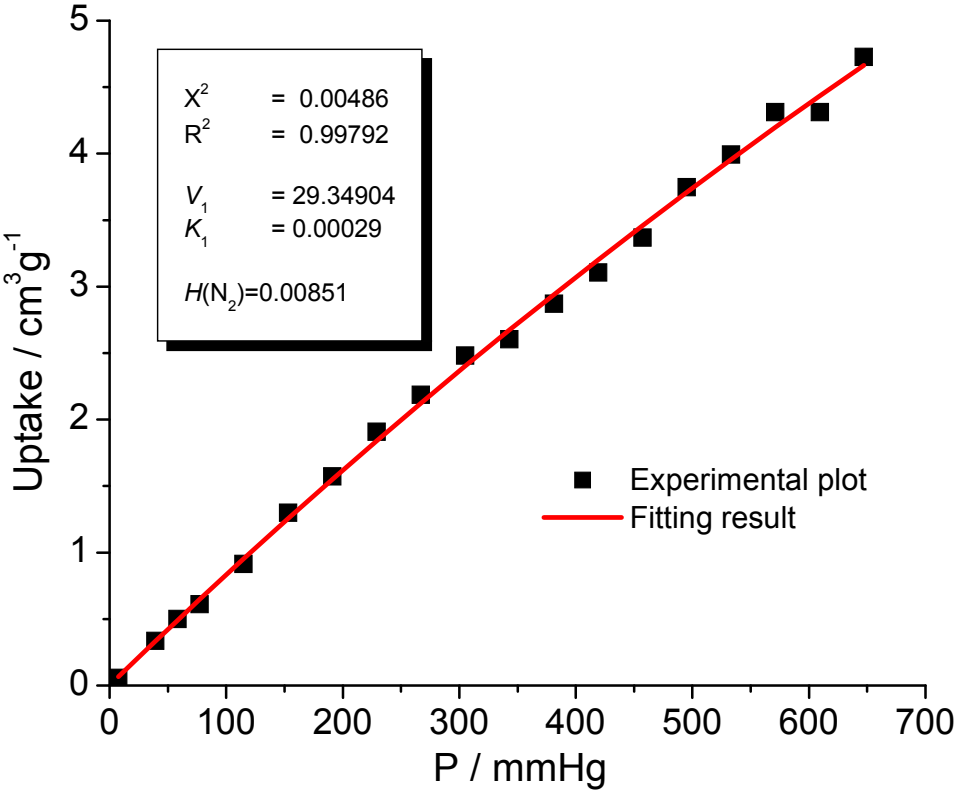

Figure S9. N_2 isotherm adsorption branch of **Pr-LOF** (filled shape) and fitting based on single Langmuir isotherm model (red line). V_1, calculated adsorbed volume of N_2; K_1, calculated affinity constants; X^2 and R^2, fitting error; H, Herry's law constant, $H(N_2)=K_1\times V_1$ ($cm^3\cdot g^{-1}\cdot mmHg^{-1}$).

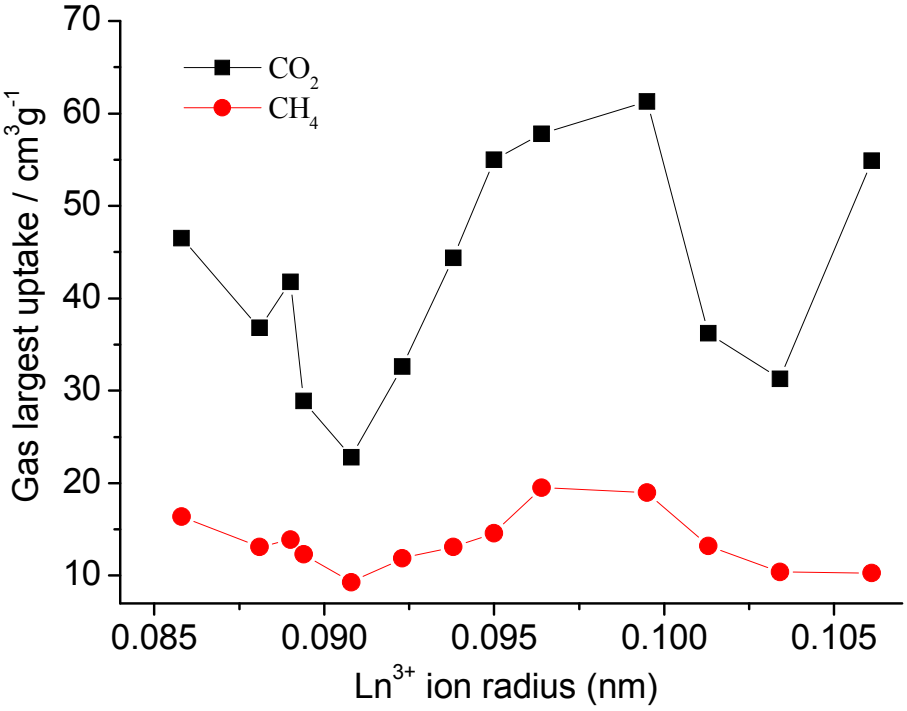

Figure S10. Relationship between lanthanide ion radius, and gas uptakes.

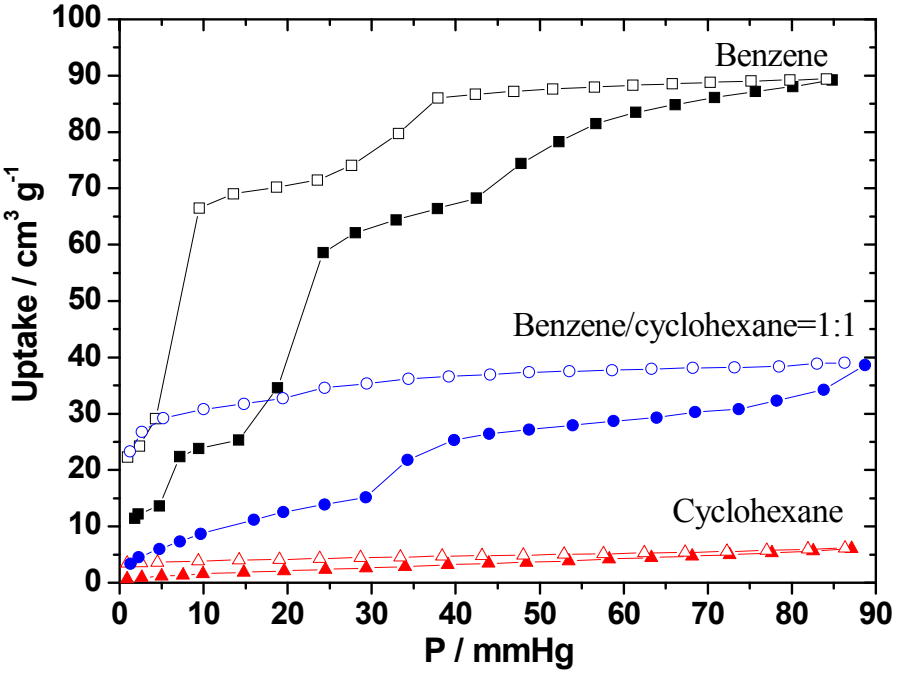

Figure S11. Ce-LOF gave the highest selectivity of benzene/cyclohexane adsorption at 298 K. The blue cycle plots show the sorption of benzene/cyclohexane mixture with volume ratio 1:1.

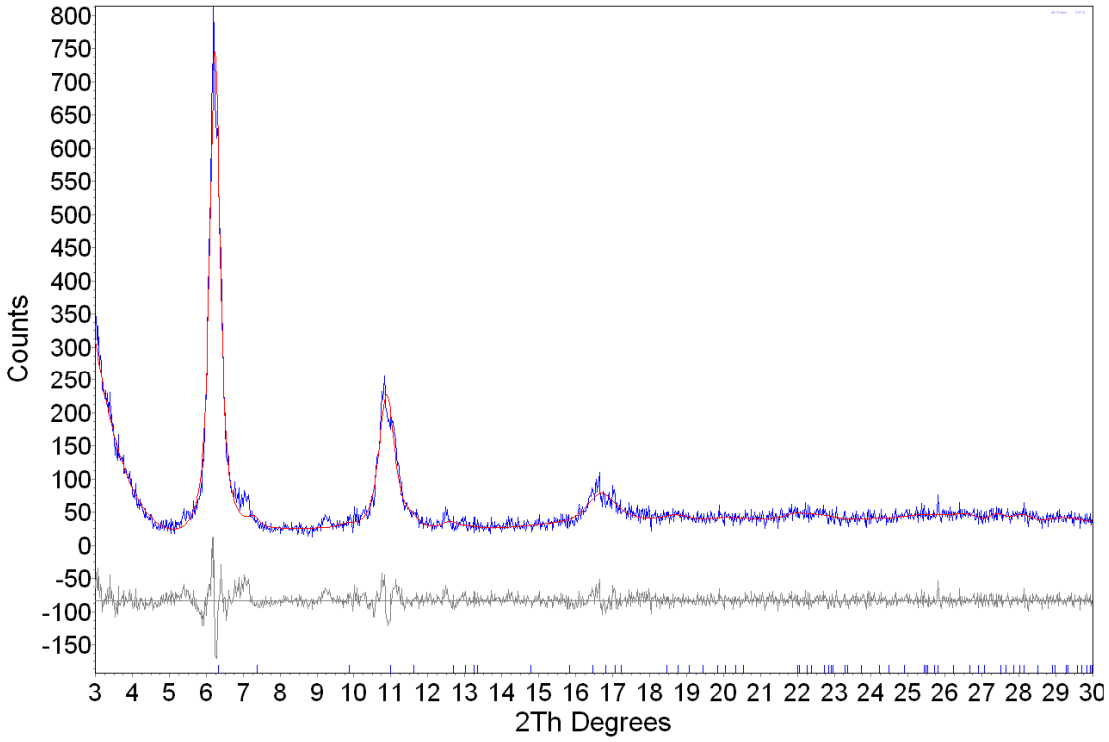

Figure 12S. Powder XRD patterns of **Nd-LOF** indexed by program TOPAS with a hexagonal $P6_122$ space group (a= 16.17(6) Å, c= 25.57(13) Å).

Table S3. Summary of gas adsorption test results.

Materials	Ln^{3+} ion radius (pm)	S_{BET} (m^2/g)	Pore volume (cm^3/g)	CO_2 uptake (cm^3/g)	CH_4 uptake (cm^3/g)
Y-LOF	89	667	0.44	41.8	13.9
La-LOF	106.1	351	0.31	54.9	10.3
Ce-LOF	103.4	363	0.32	31.3	10.4
Pr-LOF	101.3	484	0.30	36.2	13.2
Nd-LOF	99.5	477	0.29	61.3	19.0
Sm-LOF	96.4	581	0.35	57.8	19.5
Eu-LOF	95.0	426	0.30	55.0	14.6
Gd-LOF	93.8	535	0.31	44.4	13.1
Tb-LOF	92.3	158	0.13	32.6	11.9
Dy-LOF	90.8	281	0.17	22.8	9.3
Ho-LOF	89.4	233	0.14	28.9	12.3
Er-LOF	88.1	283	0.20	36.8	13.1
Yb-LOF	85.8	443	0.38	46.5	16.4

Table S4. CO_2 uptake at 273K and 1 atm of lanthanide-based MOFs.

Materials	Uptake [cm^3/g]	Ref.
$Dy(BTC)(H_2O)\cdot DMF$	189	[1]
$[Y_2(TPO)_2(HCOO)]\cdot(Me_2NH_2)\cdot(DMF)_4\cdot(H_2O)_6$	66.9	[2]
$[Eu(L)_4]^{5-}$	19.5(P/P_0=0.03)	[3]
$\{La(cpia)(2H_2O)_3\cdot 4H_2O\}_n$	23 (P/P_0=0.03)	[4]
$\{KHo(C_2O_4)_2(H_2O)_4\}_n$	21.2 (298 K)	[5]
$(Yb_4(\mu_4\text{-}H_2O)(C_{24}H_{12}N_3O_6)_{8/3}(SO_4)_2\cdot 3H_2O\cdot 10DMSO)$	220 (195 K)	[6]
Gd(TPO)	285.8 (195 K)	[7]
$Er_2(TBDC)_3(phen)_2\ 34DMF_3\ 2H_2O$	51 (195 K)	[8]
Nd(BTB)	61.3	This work

Table S5. Benzene and cyclohexane saturate uptake at 298K.

Materials	Benzene uptake (mg/g)	Cyclohexane uptake (mg/g)	Selectivity [a]
La-LOF	189.7	106.7	1.8
Ce-LOF	311.0	22.9	13.6
Pr-LOF	288.2	33.4	8.6
Nd-LOF	174.7	74.6	2.3
Sm-LOF	214.2	155.4	1.4
Tb-LOF	88.5	41.6	2.1
Dy-LOF	116.0	113.5	1.0
{[Zn(μ_4-TCNQ-TCNQ)bpy]·1.5benzene}$_n$ [b]	80	20	4
MAF-2 [c]	206	9	22.9

[a] Selectivity= Benzene uptake/ Cyclohexane uptake.
[b] Ref. 9.
[c] Ref. 10.

References:

[1] X. Guo, G. Zhu, Z. Li, F. Sun, Z. Yang and S. Qiu, *Chem. Commun*., 2006, 3172.

[2] Z.-J. Lin, Z. Yang, T.-F. Liu, Y.-B. Huang and R. Cao, *Inorg. Chem*., 2012, **51**, 1813.

[3] B. D. Chandler, J. O. Yu, D. T. Cramb and G. K. H. Shimizu, *Chem. Mater*., 2007, **19**, 4467.

[4] P. Lama, A. Aijaz, S. Neogi, L. J. Barbour and P. K. Bharadwaj, *Cryst. Growth Des*., 2010, **10**, 3410.

[5] S. Mohapatra, K. P. S. S. Hembram, U. Waghmare and T. K. Maji, *Chem. Mater*., 2009, **21**, 5406.

[6] S. Ma, X.-S. Wang, D. Yuan and H.-C. Zhou, *Angew. Chem. Int. Ed*., 2008, **47**, 4130.

[7] W. R. Lee, D. W. Ryu, J. W. Lee, J. H. Yoon, E. K. Koh and C. S. Hong, *Inorg. Chem*., 2010, **49**, 4723.

[8] H. He, D. Yuan, H. Ma, D. Sun, G. Zhang and H.-C. Zhou, *Inorg. Chem*., 2010, **49**, 7605.

[9] S. Shimomura, S. Horike, R. Matsuda and S. Kitagawa, *J. Am. Chem. Soc.*, 2007, **129**, 10990.

[10] J.-P. Zhang and X. -M. Chen, *J. Am. Chem. Soc*., 2008, **130**, 6010.